Time-Frequency Analysis of Spectrally-Notched Random FM Waveforms

Thomas J. Kramer, Shannon D. Blunt
Radar Systems Lab (RSL), University of Kansas, Lawrence, KS

***Abstract*—Various classes of random FM waveforms have recently emerged that are amenable for high-power radar transmitters while providing high dimensionality that facilitates a variety of new applications. One prominent example is the generation of transmit spectral notching to contend with dynamic radio frequency interference (RFI) for the purpose of spectrum sharing. While previous design-focused work has used the aggregate power spectrum and autocorrelation properties of these waveforms to facilitate spectrum-shaping optimization, here we examine their time-frequency characteristics to better understand the efficacy of spectral notching at different time scales. In so doing it is observed that there may be a need for different design perspectives depending on the nature of the RFI.**

Keywords—FM noise radar, waveform optimization, time-frequency analysis

I. Introduction

Radar waveforms can generally be delineated into the categories of linear and nonlinear frequency modulation (FM), phase codes, frequency codes, noise waveforms, and ultrawideband waveforms [1, 2]. Of these categories, the degree of structure in the signal varies significantly, with noise waveforms clearly possessing the least amount of structure and, therefore, the greatest freedom to maneuver. A particular sub-category of noise waveforms in which the randomness occurs via frequency modulation has recently been demonstrated to provide a variety of useful emerging capabilities (see [3] for a summary). Consequently, these FM noise (or random FM) waveforms employ enough signal structure to make them amenable to high-power transmitters while otherwise possessing the extremely high dimensionality and maneuver freedom (due to non-repetition) of traditional noise waveforms.

While the beginnings of classical noise radar are generally attributed to the work of Horton published in 1959 [4], the origins of random FM can actually be traced to a U.S. Navy patent filed by Whiteley and Adrian in 1956 [5], though it was not issued until 1980. Since that time, different system implementations and analytical attributes of random FM have been examined by Guosui, et al, throughout the 1990s [6], by Axelsson in 2004 [7], and most recently by Pralon, et al, [8, 9]. A common thread through these various efforts has been the use of white noise to drive an FM signal.

Starting with the pseudo-random optimized (PRO) FM approach in 2015 [10, 11] the University of Kansas, in collaboration with the Army Research Laboratory (ARL), the the Air Force Research Laboratory (AFRL), and the Naval Research Laboratory (NRL), has developed a variety of new classes and applications of random FM waveforms (see [3] and references within). The defining feature of these waveform classes is that, through some manner of optimization, they are able to facilitate useful shaping of the waveform's power spectrum while still retaining both the inherent randomness (providing high dimensionality) and FM structure (for high-power transmission).

Among these random FM waveform classes, the incorporation of transmit spectral notches to address dynamically changing RFI [12] presents a particularly interesting perspective with regard to spectrum shaping. Specifically, since an FM waveform, by definition, is phase-continuous and only corresponds to a single frequency at any instant in time, what attribute of this signal permits it to achieve such low spectral notch depths? For instance, better than 50 dB notch depth has been demonstrated in hardware [13, 14]. Moreover, are there time-scale dependencies to this degree of spectral suppression? Here we apply time-frequency (TF) analysis to investigate these questions.

II. Random FM Waveforms

The list of random FM waveform classes continues to grow, and thus an exhaustive analysis of their TF properties is not feasible here. Instead we evaluate the specific TF impact that spectral notching has upon them, which leads to some interesting observations. Note that, being FM, all of these waveforms are constant amplitude and continuous.

The baseline, non-optimized FM noise case studied in [5-9] is the most direct way to generate a random FM waveform. The baseband representation of any FM waveform, random or otherwise, can be expressed as

$$s(t) = \exp\left(j2\pi \int_{-\infty}^{t} f(\tau)\, d\tau \right) = \exp\big(j\theta(t) \big), \qquad (1)$$

for instantaneous frequency $f(\tau)$ of the modulating random process and $\theta(t)$ the subsequent random phase, which is continuous. In [5-9] this modulating random process was generally assumed to be Gaussian. In all cases the waveform $s(t)$ possesses a single frequency at a given instant in time.

More recent work [3] has focused on ways in which to perform spectral shaping of random FM waveforms so as to achieve lower range sidelobes on a per-waveform basis and to incorporate spectral notches on transmit [12]. Such spectral shaping cannot be achieved through simple linear filtering because doing so would involve deviating from the desirable FM structure. Thus some degree of optimization is often required, which also generally necessitates operation on an appropriately discretized version of the waveform (i.e. inclusion of "over-sampling" relative to 3-dB bandwidth so unavoidable aliasing is kept to an acceptable minimum [15]).

This work was supported by the Office of Naval Research under Contract #N00014-16-C-2029. DISTRIBUTION STATEMENT A. Approved for Public Release.

An important note at this point is with regard to global versus local optimality. While most optimization problems seek the former, the latter is actually more useful in this case. In fact, the preservation of randomness is achieved because each random initialization tends toward a (sufficiently) unique result when performing spectral shaping. Consequently, each waveform can be designed to be "good enough" while remaining distinct from the rest. This uniqueness across a set of random FM waveforms also leads to the condition whereby their individual pulse compressed range sidelobes combine incoherently during slow-time processing (thereby incurring a reduction through averaging) while the mainlobe responses still combine coherently.

The particular spectrum-shaping approach considered here is PRO-FM [10, 11], which employs alternating time/frequency projections to convert an arbitrary random FM initialization into one that approximately adheres to a desired power spectrum template. The Gaussian power spectrum is attractive because it corresponds to a Gaussian autocorrelation [16], which theoretically has no sidelobes. While this condition can only be met approximately (i.e. practical time-limited waveforms deviate somewhat from a true Gaussian power spectrum), sidelobes roughly on the order of $-20\log_{10}(BT)$ can readily be achieved [10], with BT the 3-dB time-bandwidth product. By modifying the spectral template followed by subsequent "notch deepening" methods [12-14], spectrally notched FM waveforms compatible with physical transmitters can be realized to support cognitive radar spectrum sharing.

III. Time-Frequency Transformation Review

When analyzing a time-varying or non-stationary signal, such as random FM waveforms, the time-domain representation does not clearly show what frequencies are present at a particular time. Conversely, the frequency representation does not easily describe when the particular frequencies are present in the signal. Evaluation of this relationship necessitates the use of a joint time-frequency representation [17].

TF transformations fall into one of two types: linear or nonlinear. The most commonly used linear TF transformation is the short-term Fourier transform (STFT), defined as [17]

$$\mathrm{STFT}_s(t,f)=\int_\tau [s(\tau)\,\gamma^*(\tau-t)]e^{-j2\pi f\tau}d\tau\,, \tag{2}$$

where $\gamma(t)$ is a window function with some specified time support (here we use a rectangular window whose extent is a percentage of the pulse width). Other linear TF transforms exist as well, such as the wavelet transform (with a wide variety of wavelets) [18]. Linear TF transforms generally involve a trade-off between temporal resolution and spectral resolution, which can hinder the characterization of waveforms possessing sophisticated intrapulse behavior [19].

In contrast, the distributions produced by nonlinear TF transformations, with bilinear (quadratic) being of particular interest, trade between joint time/frequency resolution ($\Delta t\,\Delta f$) and interference cross-terms [17]. Since we wish to preserve temporal and spectral resolution, we shall consider a nonlinear transform. A popular nonlinear TF representation is the Wigner-Ville transform (WVD), since many other TF transforms can be easily derived from it [18].

The WVD of waveform $s(t)$, defined mathematically as [17]

$$W_s(t,f)=\underset{\tau\to f}{\mathcal{F}}\left\{s\left(t+\tau/2\right)\,s^*\!\left(t-\tau/2\right)\right\}, \tag{3}$$

involves a quadratic TF transformation with many properties that are well-suited for analyzing signals at full temporal and spectral resolution. Integrating over the entire WVD results in the total energy of the signal, while integrating over a time (delay) marginal or a frequency marginal results in the total energy in the given delay or frequency bin. Another desirable property of the WVD is that it can be transformed into many other bilinear TF distributions either through integral transforms (e.g. Fourier) or by multiplying a kernel function into the integrand.

There are still several trade-offs that must be considered when employing the WVD to analyze signals [17]. Self-interference cross-terms arise throughout the signal's TF representation and may potentially obfuscate the signal structure, though they are needed to satisfy the marginal conditions noted above. For FM waveforms, these cross-terms are centered between "auto-terms", which are regions of constant frequency at different points in time. Cross-terms are a consequence of the quadratic superposition principle that the WVD satisfies [19]. Also, because radar waveforms cannot be both time-limited and bandlimited, we must consider infinite representation across one of the two axes. Consequently, some aliasing is expected to occur in either time or frequency. However, with adequate sampling the degree of aliasing can be kept to an acceptable minimum.

As noted above, other bilinear TF distributions can be obtained from the WVD. Applying a Fourier transform across the time axis of the WVD as [17]

$$C_s(v,f)=\underset{\tau\to v}{\mathcal{F}}\left\{W_s(t,f)\right\} \tag{4}$$

realizes the spectral correlation function (SCF), which provides a measure of the similarity between a signal and a frequency shifted version of itself within each frequency bin. While not used here, the instantaneous autocorrelation function (IAF) can likewise be obtained by applying an inverse Fourier transform to the WVD across the frequency axis [17]. Moreover, the well-known ambiguity function (AF) can also be derived from the WVD by applying both a Fourier transform across the time axis and an inverse Fourier transform across the frequency axis [17]. These four bilinear distributions (WVD, SCF, IAF, and AF) are all connected through a cycle of Fourier transforms and inverse Fourier transforms. Here we specifically consider the WVD and SCF.

One final TF transform of interest is the Radon-Wigner transform (RWT), which is obtained from the fractional Fourier transform that is defined as

$$\begin{aligned}\underset{t\to u}{\mathcal{F}^\alpha}\left\{s(t)\right\}&=\sqrt{\frac{1-j\cot(\alpha)}{2\pi}}\exp\left\{j0.5\cot(\alpha)u^2\right\}\\&\quad\times\int_{-\infty}^{\infty}\exp\left\{j\left(0.5\cot(\alpha)t^2-\csc(\alpha)ut\right)\right\}\,s(t)\,dt,\end{aligned} \tag{5}$$

where $\cot(\cdot)$ and $\csc(\cdot)$ are the cotangent and cosecant operations, respectively, and the α and u variables correspond to the angle and radial variables of the transform. Specifically, α is the angle of rotation in the time-frequency domain and u is the generalized marginal (see page 284 of [17] for details on marginals). Based on (5), the RWT is computed as

$$R_s(\alpha,u) = \underset{t \to u}{\mathcal{F}^{\alpha}} \left\{ s(t)\, s^*(t) \right\} \text{ for } 0^\circ \leq \alpha \leq 180^\circ . \qquad (6)$$

The specific portion of the RWT response from (6) for which $\alpha = 90^\circ$ then denotes the usual Fourier transform of the argument. These various TF transforms will be used to provide greater insight into the structure of random FM waveforms, particularly those possessing spectral notches.

IV. Time-Frequency Analysis of Random FM Waveforms

It has been shown [12-14] that spectrally notching random FM waveforms can realize notch depths better than 50 dB while retaining the FM structure that is amenable to high-power transmitters. Figure 1 illustrates an experimental loopback capture example of this capability when shaping the power spectrum to be Gaussian for a 2 μs random FM pulse having a 3-dB bandwidth of 200 MHz, with and without a spectral notch.

It is interesting to consider the WVD of these same waveforms via (3), which are depicted in Figs. 2 and 3. Specifically, despite the prominent spectral notch in Fig. 1, the WVD results for waveforms with and without a spectral notch are virtually indistinguishable. In fact, even knowing that the spectral notch resides in the 60 to 90 MHz interval, there is no evidence of its existence at that interval in Fig. 3.

It is possible to discern some indications of a spectral notch if we average the WVD responses over a sufficient number of unique waveforms (with the same spectral notch location). Figure 4 shows that direct averaging of the WVD responses of 100 notched random FM waveforms (also loopback captured) reveals the inner edge of the spectral notch, though the outer edge is not as clear. The notch in Fig. 4 also appears to be quite shallow, in contrast to the almost 50 dB notch depth in Fig. 1 that depicts the power spectrum measured over the entire pulse.

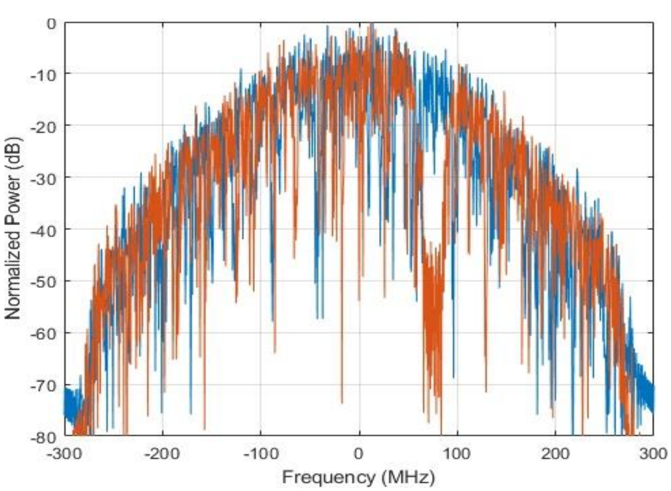

Fig 1. Baseband power spectrum of random FM (blue trace) and spectrally notched random FM (orange trace) waveforms experimentally captured in loopback

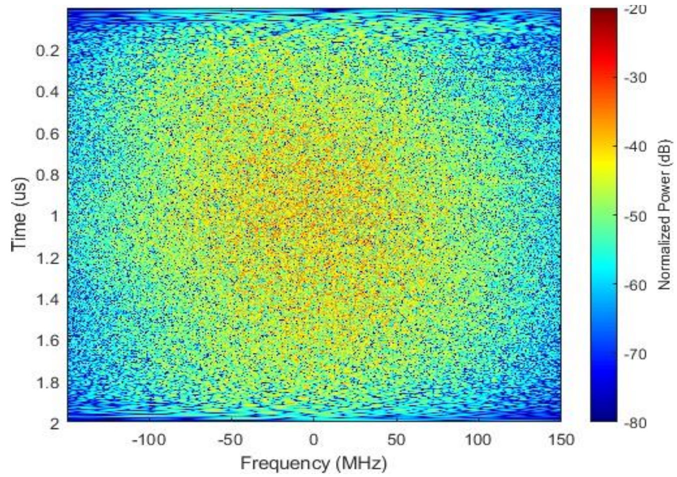

Fig. 2. WVD of a single random FM waveform (loopback)

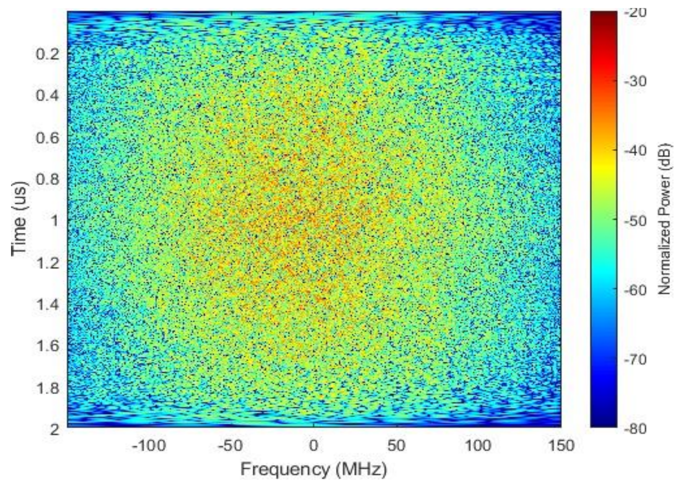

Fig. 3. WVD of a single spectrally notched random FM waveform (loopback)

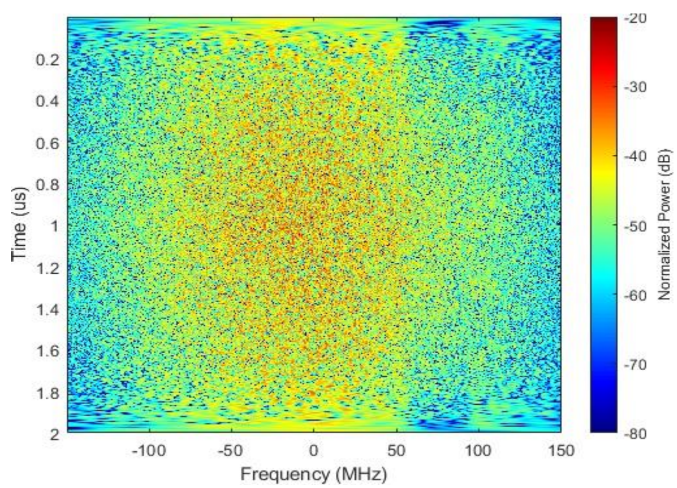

Fig. 4. Averaged WVD over 100 notched random FM waveforms (loopback)

The main reason for this disparity between instantaneous spectral content (as measured by WVD) and aggregate spectral content arises from how the spectral notch is actually formed. Simply put, the signal content within the frequency interval of the notch is combining in a way to facilitate a cancellation effect over the pulse, which is a rather different phenomena than avoiding placement of any signal energy in this frequency interval.

One way to demonstrate this cancellation effect is by using the SCF, which involves performing a Fourier transform over the time axis of the WVD response from (3), thereby converting the time domain into the fast-time Doppler domain. Consequently, the frequency content is evaluated over the pulse width as a whole.

Figures 5 and 6 illustrate the resulting SCF responses for the same two waveforms depicted in Figs. 2 and 3. This frequency versus Doppler perspective clearly shows the spectral notch in Fig. 6, while also revealing that the notch location shifts according to fast-time Doppler. Thus, under conditions of scatterers possessing high radial velocity (e.g. helicopter blades) and/or high Doppler sensitivity such as that experienced at mm-wave bands, maintaining the notch spectral location may require further consideration depending on the radar's operating concept. Moreover, we can infer that the time-scale over which the spectral notch is evaluated does indeed matter.

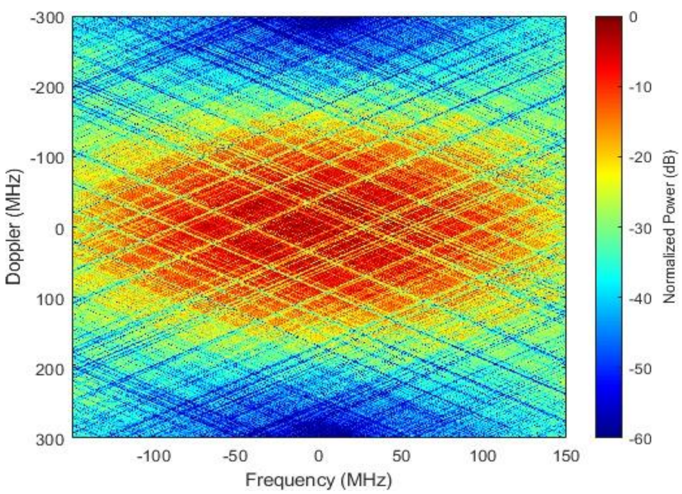

Fig. 5. SCF of a single random FM waveform (loopback)

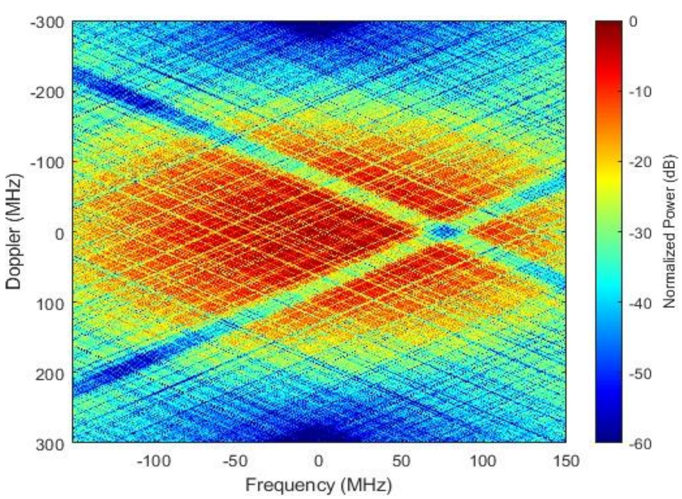

Fig. 6. SCF of a single notched random FM waveform (loopback)

This time-scale dependence is further emphasized when considering the RWT response from (6) that is shown in Fig. 7. As noted above, $\alpha = 90°$ corresponds to the Fourier transform response and, consequently, the spectral notch is clearly visible in that regime. However, other values of α that relate to other portions of the time-frequency space do not appear to preserve the notch. We can again infer that the time-scale over which the spectral notch is evaluated determines the efficacy with which those particular frequencies are avoided.

Finally, consider the application of the STFT from (2) to the notched random FM waveform at two different time-scales. Figures 8 and 9 first show the STFT response when the time window is 10% of the pulse width. Here the notch is clearly visible, albeit obviously a bit narrower and slightly shallower than indicated in Fig. 1 when observed over the pulse width as a whole. However, at this time-scale we can easily say that the spectral notch does clearly exist.

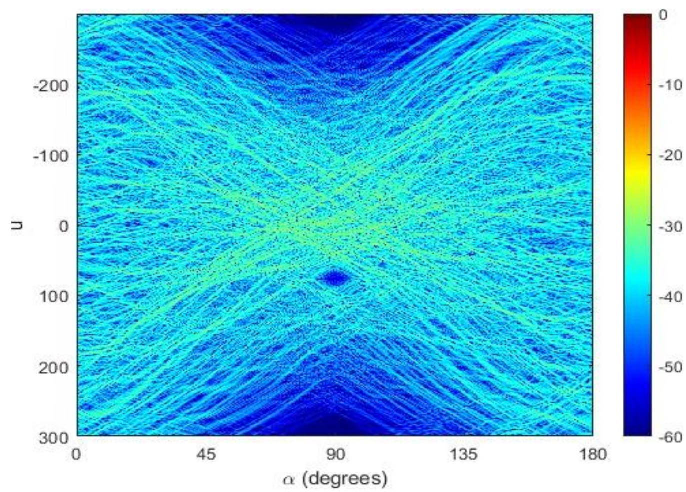

Fig. 7. RWT of a single notched random FM waveform (loopback)

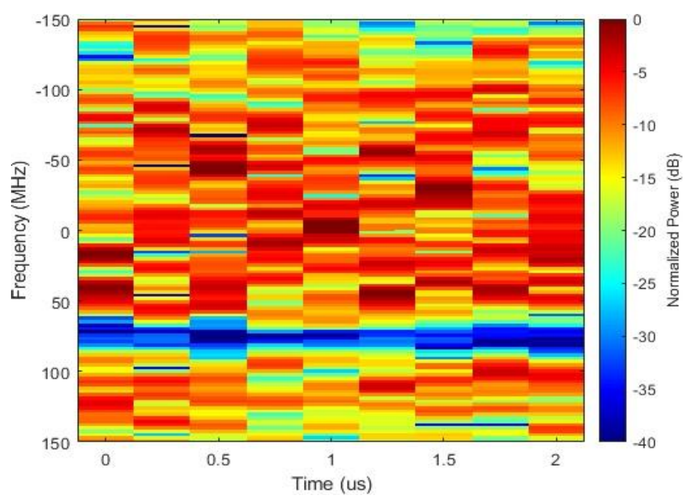

Fig. 8. STFT response of a single notched random FM waveform (loopback) for a 10% time window

In contrast, Figs. 10 and 11 illustrate the STFT response when the time window is 2% of the pulse width. Now the spectral notch can be vaguely observed traversing across Fig. 10, though it is certainly not the consistent presence shown in Fig. 8 for the longer STFT time window. From the perspective of a few STFT response time segments in Fig. 11, however, it would be difficult to justify that a spectral notch is actually present. Simply put, from the standpoint of another spectrum user in the same band as the radar, the efficacy of spectral notching performed by the radar strongly depends on the operational time-scale of the other spectrum user.

Further, the depth of the notch from a TF perspective can be assessed by varying the width of the STFT window. Figure 12 shows the improvement in (perceived) relative notch depth as the window size increases. This result is also visually demonstrated in Fig. 13, where the frequency marginals (sum of the spectrogram across time) are plotted for different window sizes.

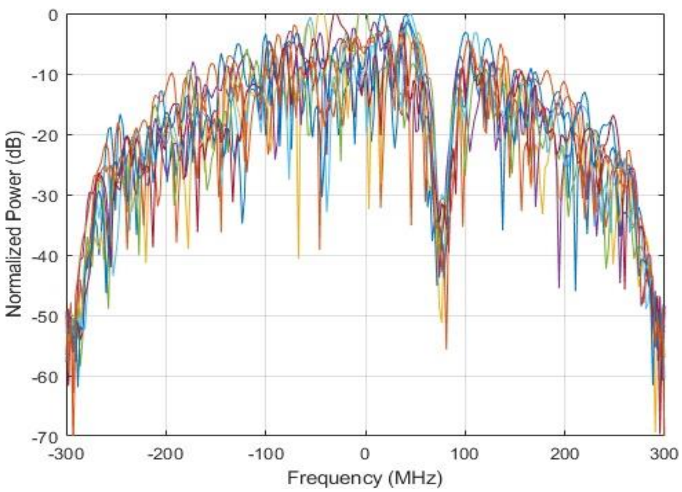

Fig. 9. STFT response of a single notched random FM waveform (loopback) for a 10% time window; view of a few individual time segments

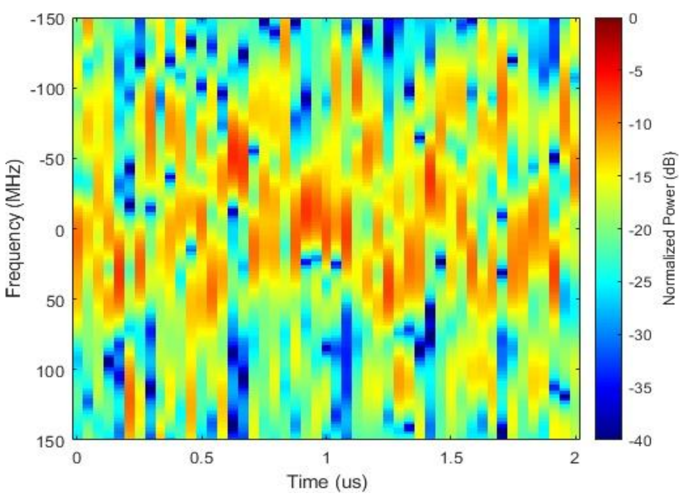

Fig. 10. STFT response of a single notched random FM waveform (loopback) for a 2% time window

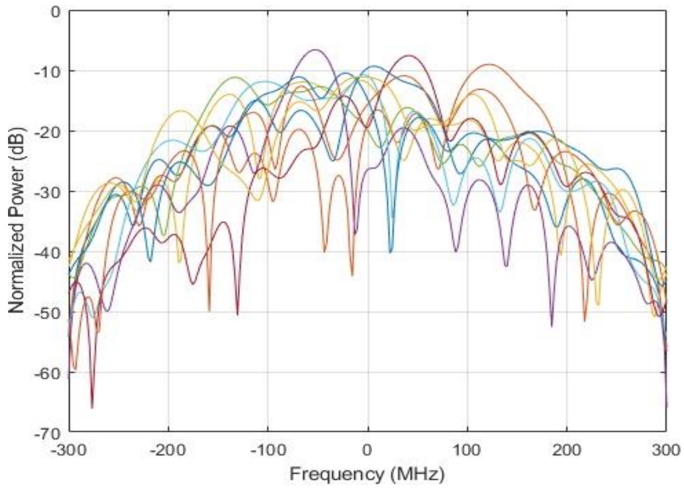

Fig. 11. STFT response of a single notched random FM waveform (loopback) for a 2% time window; view of a few individual time segments

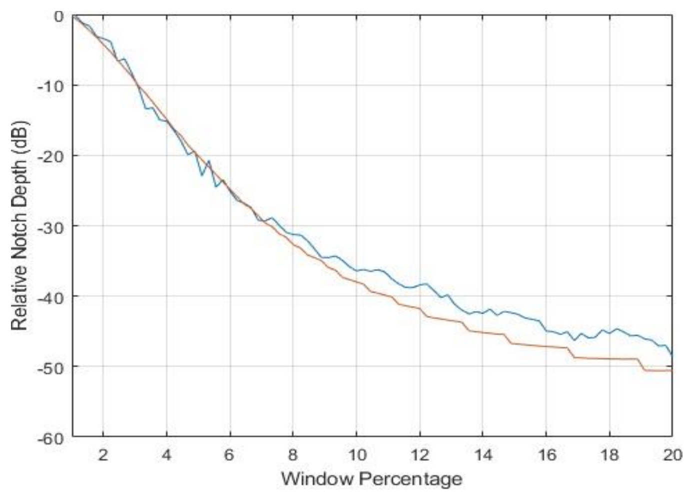

Fig. 12. Relative notch depth versus window size as a percentage of waveform temporal extent (loopback), both for a single notched random FM waveform (blue trace) and averaged over 1,000 unique waveforms (orange trace).

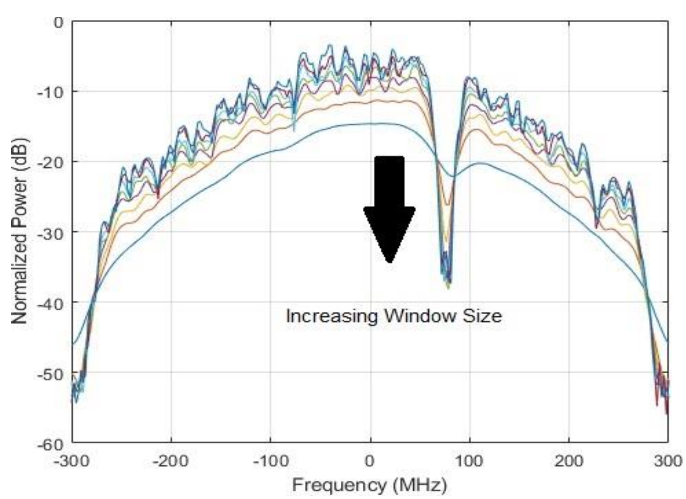

Fig. 13. Frequency marginals of various spectrogram window sizes for an arbitrary notched random FM waveform (loopback), with the relative notch depth improving as the window size increases.

V. TRADITIONAL FM DESIGN PERSPECTIVE

The TF outcome for notching might seem to represent a departure from the well-known principle of stationary phase (PSP) that is a cornerstone of traditional FM waveform design. The PSP describes an inverse relationship between the rate of frequency change (i.e. chirp rate) and spectral density, defined at frequency f_k, as [1,20]

$$|U(f_k)|^2 \approx 2\pi \frac{g^2(t_k)}{|\phi''(t_k)|} \tag{7}$$

where $\phi''(t_k)$ is the chirp-rate at corresponding time t_k and $g(t_k)$ is the amplitude envelope of the pulse (here a constant since the waveform is FM). Within this context, the instantaneous frequency as a function of time $f(t)$ is related to the group time-delay function $T(f)$ as [1]

$$f(t) = T^{-1}(f)\ , \tag{8}$$

where

$$f(t) = \frac{1}{2\pi}\frac{d\phi}{dt} \tag{9}$$

and

$$T(f) = -2\pi\frac{d\phi}{df}\ . \tag{10}$$

When the instantaneous frequency in (7) is monotonic, the inverse function of group delay exists and the relationship between group time delay and instantaneous frequency is one-to-one.

However, when the instantaneous frequency is non-monotonic, such as in the case of random FM waveforms, this relationship is no longer one-to-one and thus the inverse function does not exist. Consequently, the principle of stationary phase does not hold for random FM waveforms. In other words, we cannot necessarily expect to form spectral notches by simply "chirping quickly" through the notch interval, which is why the results observed here indicate that cancellation is necessary to achieve significant notch depth.

VI. CONCLUSIONS

Random FM waveforms have been experimentally demonstrated as a viable means with which to realize cognitive radar spectrum sharing through the formation of transmit spectral notches. Here these notches have been evaluated from a time-frequency perspective, where it is found that the time-scale over which the notch is assessed has a significant impact on the observed notch depth. Moreover, the principle of stationary phase does not appear to apply for these waveforms, with the notch formation instead achieved through means of cancellation over the pulse width. Thus these results imply that the relative time-scales between the radar and RFI should be considered when designing notched waveforms.

REFERENCES

[1] N. Levanon, E. Mozeson, *Radar Signals*, Wiley-IEEE Press, 2004.

[2] S.D. Blunt, E.L. Mokole, "Overview of radar waveform diversity," *IEEE Aerospace and Electronic Systems Mag.*, vol. 31, no. 11, Nov. 2016.

[3] S.D. Blunt, J.K. Jakabosky, C.A. Mohr, P.M. McCormick, et al, "Principles & applications of random FM radar waveform design," to appear in *IEEE Aerospace & Electronic Systems Magazine*.

[4] B.M. Horton, "Noise-modulated distance measuring systems," Proc. IRE, vol. 47, no. 5, pp. 821-828, May 1959.

[5] T.B. Whiteley, D.J. Adrian, "Random FM autocorrelation fuze system," U.S. Patent #4,220,952, issued Sept. 2, 1980, application filed Feb. 17, 1956.

[6] L. Guosui, G. Hong, Z. Xiaohua, S. Weimin, "The present and future of random signal radars," *IEEE Aerospace & Electronic Systems Mag.*, vol. 12, no. 10, pp. 35-40, Oct. 1997.

[7] S.R.J. Axelsson, "Noise radar using random phase and frequency modulation," *IEEE Trans. Geoscience & Remote Sensing*, vol. 42, no. 11, pp. 2370-2384, Nov. 2004.

[8] L. Pralon, B. Pompeo, J.M. Fortes, "Stochastic analysis of random frequency modulated waveforms for noise radar systems," *IEEE Trans. Aerospace & Electronic Systems*, vol. 51, no. 2, pp. 1447-1461, Apr. 2015.

[9] L. Pralon, G. Beltrao, B. Pompeo, M. Pralon, J.M. Fortes, "Near-thumbtack ambiguity function of random frequency modulated signals," *IEEE Radar Conf.*, Seattle, WA, May 2017.

[10] J Jakabosky, S. D. Blunt, B. Himed, "Waveform design and receive processing for nonrecurrent nonlinear FMCW radar," *IEEE Intl. Radar Conf.*, Washington, DC, May 2015.

[11] J. Jakabosky, S.D. Blunt, B. Himed, "Spectral-shape optimized FM noise radar for pulse agility," *IEEE Radar Conf.*, Philadelphia, PA, May 2016.

[12] B. Ravenscroft, et al, "Experimental demonstration and analysis of cognitive spectrum sensing & notching," *IET Radar, Sonar & Navigation*, vol. 12, no. 12, pp. 1466-1475, Dec. 2018.

[13] C.A. Mohr, S.D. Blunt, "Analytical spectrum representation for physical waveform optimization requring extreme fidelity," *IEEE Radar Conf.*, Boston, MA, Apr. 2019.

[14] C.A. Mohr, J.W. Owen, S.D. Blunt, C.T. Allen, "Zero-order reconstruction optimization of waveforms (ZOROW) for modest DAC rates," submitted to *IEEE Intl. Radar Conf.*, Washington, DC, Apr. 2020.

[15] S.D. Blunt, M. Cook, J. Jakabosky, J. de Graaf, E. Perrins, "Polyphase-coded FM (PCFM) radar waveforms, part I: implementation," *IEEE Trans. Aerospace & Electronic Systems*, vol. 50, no. 3, pp. 2218-2229, July 2014.

[16] A. Johnston, "Improvements to a pulse compression radar matched filter," *Radar & Electronic Engineer*, vol. 53, no. 4, pp. 138-140, Apr. 1983.

[17] B. Boashash, *Time-Frequency Signal Analysis and Processing*, 2016.

[18] L. Cohen, "Time-frequency distributions – a review," *Proc. IEEE*, vol. 77, no. 7, Jul. 1989.

[19] F. Hlawatsch, G.F. Boudreaux-Bartels, "Linear and quadratic time-frequency signal representations," *IEEE Signal Processing Magazine*, vol. 9, no. 2, pp. 21-67, Apr. 1992.

[20] E.N. Fowle, "The design of FM pulse compression signals," *IEEE Trans. Information Theory*, vol. 10, no. 1, pp. 61-67, Jan. 1964.